

Strain recovery of post-yield compressed semicrystalline poly(butylene terephthalate)

Alessandro Pegoretti^{a,*}, Stefano Pandini^b, Theonis Ricco^b

^a Department of Materials Engineering and Industrial Technologies and INSTM Research Unit, University of Trento, via Mesiano 77, 38050 Trento, Italy

^b Department of Chemistry and Physics for Engineering and Materials and INSTM Research Unit, University of Brescia, via Valotti 9, 25123 Brescia, Italy

Received 29 November 2005; received in revised form 17 May 2006; accepted 6 June 2006

Available online 7 July 2006

Abstract

Cubic specimens of a semicrystalline poly(butylene terephthalate) (PBT) have been compressed up to post-yield deformation levels with a fast ($3.0 \times 10^{-2} \text{ s}^{-1}$) and a slow ($1.5 \times 10^{-4} \text{ s}^{-1}$) strain rate at three different temperatures (25 °C, 45 °C, and 100 °C, i.e. below, close and above the glass transition temperature of the material, T_g , respectively). Differently from literature results reported for amorphous polymers, semicrystalline PBT shows that, after a post-yield deformation, recovery occurs also at temperatures higher than T_g , and that an irreversible deformation, ε_{irr} , is set in the material. The irreversible strain component has been evaluated as the residual deformation after a thermal treatment of 1 h at 180 °C.

After unloading, isothermal strain recovery has been monitored for time periods of 1 h at various temperatures. From the obtained data, strain recovery master curves have been constructed by a time–temperature superposition scheme. The features of the recovery process for the various deformation conditions have been analysed. In particular, it appears that specimens deformed below T_g show a lower irreversible component, whereas, when deformed above T_g , they display a higher irreversible deformation and a slower recovery process. Moreover, the effect of deformation rate appears particularly marked for samples deformed above T_g .

© 2006 Elsevier Ltd. All rights reserved.

Keywords: Strain recovery; Deformation; Poly(butylene terephthalate)

1. Introduction

Post-yield deformation behaviour of polymers has been extensively studied by several different methods, including calorimetric techniques [1–21], and measurements of dimensional variations after unloading (strain recovery) [3,4,7,11,15,16,19,20,22–41]. In recent years, many efforts have been also focused on understanding the mechanical behaviour of highly deformed semicrystalline polymers by X-ray diffraction studies regarding the evolution of crystallographic texture [42–50]. Generally speaking, the deformation of polymers at high strain levels is always accompanied by changes in their microscopic structure that result in an alteration of the material

state; after the applied load is released, specimens attempt to revert to their un-deformed state, eventually recovering the original shape. As pointed out by Moore and Turner [51], recovery tests were usually less intensively adopted to investigate the viscoelastic or viscoplastic behaviour of polymeric materials. In fact, more common tests like creep and stress relaxation are preferred. Nevertheless, the strain recovery test has revealed itself as a powerful method for indicating the presence of both reversible and irreversible features in the deformation of polymeric materials [3,4,7,11,15,16,19,20,22–41].

Amorphous polymers deformed in the glassy state have been proven to undergo a complete dimensional recovery in short times when heated to or above their glass transition temperature (T_g), even when deformed at high strain levels [4,22,23,27,29,36,39]. To our knowledge, the only evidence of a permanent (even if very small) deformation in amorphous

* Corresponding author. Tel.: +36 0461 882452; fax: +39 0461 881977.

E-mail address: alessandro.pegoretti@ing.unitn.it (A. Pegoretti).

polymers deformed in the glassy state has been observed by Nanzai in polystyrene [52]. On the basis of a time–temperature superposition approach, Quinson et al. [27] were able to obtain a room temperature strain recovery master curve for amorphous polymers such as poly(methylmethacrylate) (PMMA), polystyrene (PS), and polycarbonate (PC), deformed in the glassy state well beyond their yield points. On such curves, two non-elastic strain components, one named *anelastic* and the other one, named *plastic*, could be distinguished by their characteristic ranges of recovery time. For PMMA at 20 °C, the *anelastic* component resulted in recovery over a large time interval (at least 10 decades) spanning from very short times to some 10^{10} s [27]. On the other hand, the so-called *plastic* component recovers over a range of time of about two decades, which resulted to be located around one billion years for PMMA at 20 °C [27]. In amorphous polymers the phenomenon of strain recovery has been interpreted in various ways according to different molecular models, such as the state transition and conformational change theories (Eyring, Robertson, and others), free volume theories (Rush and Beck), dislocations/disclinations theories (Bowden and Raha, and Argon) and segmental motion theories (Yannas and Stachurski). A description of the above mentioned theories is clearly beyond the scope of the present paper, and the interested reader is addressed to the comprehensive review of Stachurski [53].

Semicrystalline polymers present a more complex structure due to the presence of both amorphous and crystalline domains, where the amount of crystallinity may vary from 10% to 90% in commercially available materials. Their strain recovery behaviour is markedly different from those of amorphous polymers. In fact, when deformed in the post-yield region at temperatures lower than their melting point, semicrystalline polymers evidence significant discrepancies from the behaviour of fully amorphous polymers. Some peculiar aspects of semicrystalline polymers are the extension of the strain recovery processes at temperatures much higher than T_g [19,20,22,23,26,31,34], and the appearance of a certain irreversible deformation, even when heated at temperatures much higher than T_g and within a few degrees of the melting point [20,22,23,34]. This research group recently studied the strain recovery behaviour of highly deformed semicrystalline polymers such as nylon-6 (PA6), poly(ethylene terephthalate) (PET), and poly(ethylene 2,6-naphthalenedicarboxylate) (PEN) tested in tension [19,34], and of poly(butylene terephthalate) (PBT) tested in compression [20]. Similar to amorphous polymers [27,29], the strain recovery data have been treated according to a time–temperature superposition approach, thus obtaining strain recovery master curves. Such approach clearly evidenced the different kinetics of strain recovery in semicrystalline polymers with respect to amorphous ones. In particular, by contrast to the glassy polymers, our results did not allow to distinguish the existence of different non-elastic strain components on a time basis. Moreover a real irreversible strain component has been observed for PBT starting from relatively low compression levels (of about 10%) and on PEN at a 20% elongation.

Aim of the present work is to provide some further insights towards the understanding of the strain recovery processes in semicrystalline polymers. In particular, attention has been focused on the effects of strain rate and deformation temperatures on the recovery behaviour of highly compressed semicrystalline PBT.

2. Experimental

2.1. Specimens preparation

Cubic specimens ($5.5 \times 5.5 \times 5.5$ mm³) of semicrystalline PBT (crystallinity content $X_c = 38\%$, $T_g = 47$ °C, melting temperature $T_m = 230$ °C) were machined from injection moulded rectangular bars ($60 \times 12 \times 6$ mm) of Raditer B N 100 kindly supplied by Radici Novacips SpA (Villa d'Ogna, Bergamo, Italy). Due to possible specimens' anisotropy, attention was paid to deform the cubic sample always along the same direction, i.e. perpendicular to the longest dimensions of the bars. All specimens were treated for 3 h at 190 °C under vacuum and slowly cooled down in an oven in order to release thermal stresses and uniform their thermal history.

2.2. Specimen deformation

An electromechanical testing machine (Instron, model 4502) was used to perform loading–unloading cycles in uniaxial compression under displacement control. Testing under compression mode was chosen in order to avoid plastic instability phenomena, such as necking, frequently occurring in tensile tests, that can lead to heterogeneous deformation [41]. The surfaces of the compression plates in contact with specimens were accurately oil-lubricated in order to minimize end-friction. Any alteration of the specimen behaviour can be excluded by considering the small quantity of oil as well as the limited time of contact with the PBT, which is known to be a polymer with a good chemical resistance. All tests have been performed in a thermostatic chamber (Instron, model 3119) permitting a temperature control within ± 1 °C. Specimens were subjected to a loading ramp up to two different values (15% and 30%) of the applied engineering deformation (ϵ_0). For the higher deformation level, tests were performed at three different deformation temperatures ($T_{def} = 25$ °C, 45 °C, and 100 °C), and at two cross-head speeds, V_{load} . In particular, *slow* and *fast* deformation conditions, at 0.05 mm/min (i.e. a nominal strain rate of 1.52×10^{-4} s⁻¹) and 10 mm/min (i.e. a nominal strain rate of 3.03×10^{-2} s⁻¹), respectively, were chosen. No higher cross-head speeds were adopted to avoid adiabatic heating of the sample [54]. Unloading of the sample was always performed with the compression plates rapidly moving apart at $V_{unload} = 500$ mm/min.

2.3. Strain recovery measurement

After unloading, the deformed specimen was positioned in a small thermostatic chamber, equipped with a PID control and a thermocouple sensor located in the proximity of the

specimen, permitting a temperature control within ± 1 °C. An engineering residual deformation, ϵ_{res} , was evaluated as:

$$\epsilon_{\text{res}} = \frac{h_0 - h}{h_0} \quad (1)$$

where h_0 and h are the initial and the actual specimen heights, respectively. Values of h were monitored by a digital micrometer Mitutoyo Digimatic 543-250 B with a resolution of 1 μm and connected to a computer that permitted to record data at a maximum sampling rate of 1 pt/s.

The isothermal recovery process was monitored for a standard period of 1 h at various temperatures in the range from 25 °C up to 130 °C. A schematic draw of the data acquisition set-up is sketched in Fig. 1. A good measurement of the sample height could be achieved since the specimen's top and bottom surfaces were still flat and parallel after the unloading stage; the specimen presented only slight barrelling effects on the lateral contour.

Isothermal recovery curves were then shifted along the time scale with respect to a reference temperature (T_0) till a best superposition, so that a recovery master curve was obtained for the recovery process at $T = T_0$. The shift factor, denoted as a_T , is clearly a temperature-dependent quantity, since each isothermal curve has to be shifted of an increasing amount on the time scale as the difference between the recovery temperature and the reference temperature increases. In our attempt to build a recovery master curve for each of the various deformation conditions examined, the shifts factors were all referred to a reference temperature equal to the deformation temperature.

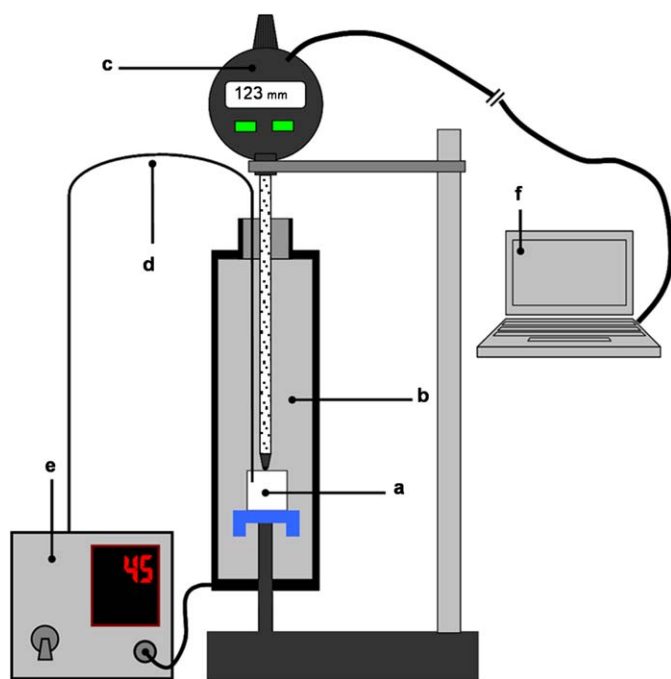


Fig. 1. Recovery data acquisition system: (a) cubic PBT specimen, (b) oven, (c) digital micrometer, (d) thermocouple sensor, (e) PID device for temperature control, and (f) computer for data acquisition.

The recovery master curves were built by means of a *single-sample* procedure proposed by Quinson et al. [27] by using the same strained specimen to measure a 1 h recovery segment for each test temperature. After each isothermal step the temperature was raised by 1.0 °C and another isothermal curve was acquired, until no further detectable recovery was observed. A standard conditioning time of 3 min was adopted in order to allow the sample to reach the temperature of the cell. In some cases, a better superposition of the isothermal curves was achieved by using two specimens recovering at various temperatures differing by 5 °C. Experimental data were corrected by PBT thermal expansion by considering a literature value of its linear thermal expansion coefficient equal to $7.4 \times 10^{-5} \text{ C}^{-1}$ [55].

An estimation of the residual deformation after unloading, ϵ_{res0} , was calculated by measuring the height of the specimen immediately at the end of the loading–unloading cycle.

An irreversible strain component, ϵ_{irr} , was arbitrarily defined as the residual deformation after a thermal treatment at 180 °C for 1 h. On the basis of differential scanning calorimetry (DSC) information, this temperature is the highest allowable before entering the melting region of this material [20,21]. It is worth saying that this residual deformation can be plausibly considered as truly irreversible, since longer thermal treatments did not induce further strain recovery, and DSC tests on treated specimens did not evidence exothermal signals related to a residual strain recovery process [21]. Besides this non-recoverable part of the deformation, the deformation that recovers instantaneously after unloading is defined as elastic deformation and is evaluated as $\epsilon_{\text{el}} = \sigma/E_u$, E_u being the unrelaxed modulus and σ the stress at the applied deformation level, ϵ_0 [20]. A third part, representing the recovery that does not take place instantaneously, and designated as non-elastic reversible component, ϵ_{ner} , can be evaluated by subtracting the elastic and irreversible strain components from the total applied deformation ($\epsilon_{\text{ner}} = \epsilon_0 - \epsilon_{\text{el}} - \epsilon_{\text{irr}}$).

3. Results and discussion

3.1. Recovery experiments

The typical appearance of a strain recovery experiment is reported in Fig. 2, for a specimen *slowly* compressed ($V_{\text{load}} = 0.05 \text{ mm/min}$) at room temperature up to 30% deformation. The figure shows different isothermal curves and the master curve obtained after shifting these curves to a reference temperature $T_0 = 25$ °C. The master curve is plotted over a reduced time scale t_{rec}/a_T , where a_T is the shift factor. In the inset of Fig. 2, the stress–strain loading–unloading curve is reported. After unloading, an initial value of the residual deformation, ϵ_{res0} , can be detected. The non-elastic reversible part, ϵ_{ner} , of the residual deformation recovers during time, and the process is thermally activated, as evidenced by the traces of the recovery curves collected within the experimental window of 1 h at various temperatures T_{rec} . Contrary to glassy polymers, the strain recovery process extends up to temperatures well above T_g of the amorphous phase [20]. This

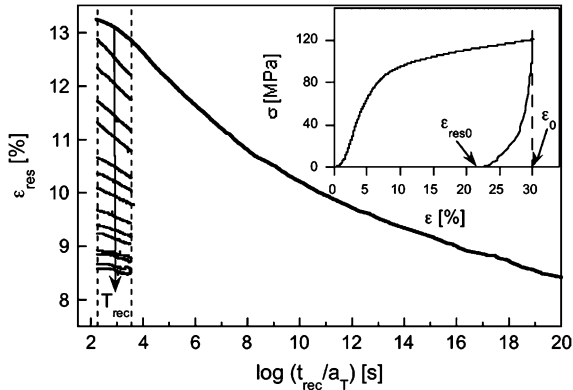


Fig. 2. Isothermal strain recovery data (thin lines) recorded within an experimental window of 1 h at temperature steps of 5 °C in the range from 25 °C up to 95 °C. The resulting strain recovery master curve (thick line) refers to a temperature of 25 °C. The inset shows the stress–strain loading–unloading curve at $V_{load} = 0.05$ mm/min up to $\epsilon_0 = 30\%$.

phenomenon could be tentatively ascribed to the presence of a mobility gradient due to the interphase between the crystalline domains and the amorphous regions [19,20,34,56,57]. Fig. 3a and b reports the strain recovery master curves of specimens *quickly* (solid lines) or *slowly* (dashed lines) compressed up to $\epsilon_0 = 15\%$ and $\epsilon_0 = 30\%$, respectively. The deformation temperature is 25 °C and hence below T_g of the amorphous phase. It is interesting to observe that the initial residual deformation,

after unloading and conditioning at the test temperature, is practically independent of the loading rate. On the other hand, the evolution of recovery master curves is clearly dependent on the loading rate. In fact, at both the investigated deformation levels, the kinetics of strain recovery results is faster for specimens *slowly* deformed in comparison with specimens *quickly* deformed.

The strain recovery process has also been investigated on specimens *quickly* or *slowly* deformed at temperatures equal ($T_{def} = 45$ °C) or higher ($T_{def} = 100$ °C) than the T_g of the amorphous regions, and the corresponding recovery master curves are reported in Fig. 4a and b, respectively. It is interesting to observe that the curves obtained at $T_{def} = 45$ °C are substantially independent of the deformation rate for a large time interval up to about $\log(t_{rec}/a_T) = 10$, while for longer times the strain recovery appears to be more rapid for the *slowly* deformed specimens. The overall picture changes when the deformation temperature largely exceeds T_g . In fact, for specimens deformed at $T_{def} = 100$ °C, the residual deformation after unloading and conditioning at the test temperature is much higher for specimens *slowly* deformed with respect to those *quickly* deformed. This behaviour could be explained by considering the occurrence of a viscous flow that is more pronounced when the time-under-load increases (i.e. in case of a *slow* deformation). Except this difference, the recovery process follows the trend previously observed on the specimens

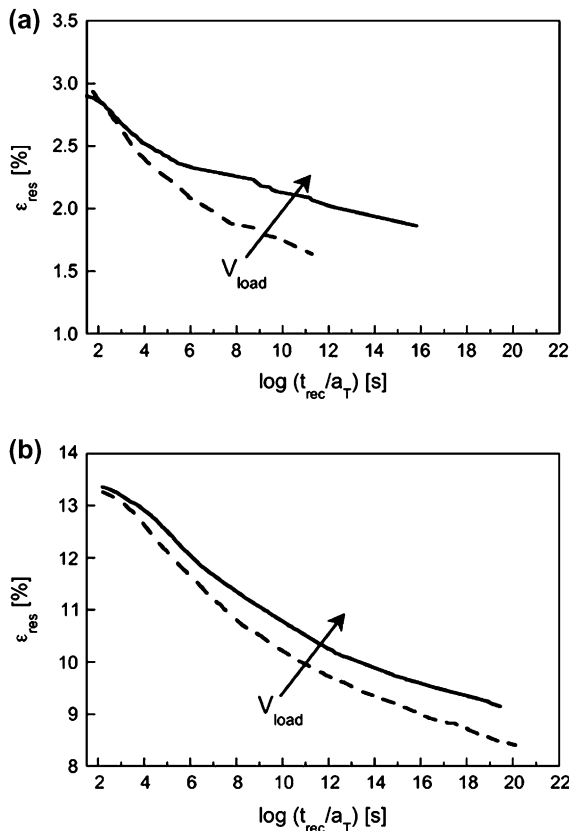


Fig. 3. Strain recovery master curves, referred to a temperature of 25 °C, for specimens deformed at 25 °C and at $V_{load} = 10$ mm/min (solid lines) or $V_{load} = 0.05$ mm/min (dashed lines) up to (a) $\epsilon_0 = 15\%$, and (b) $\epsilon_0 = 30\%$.

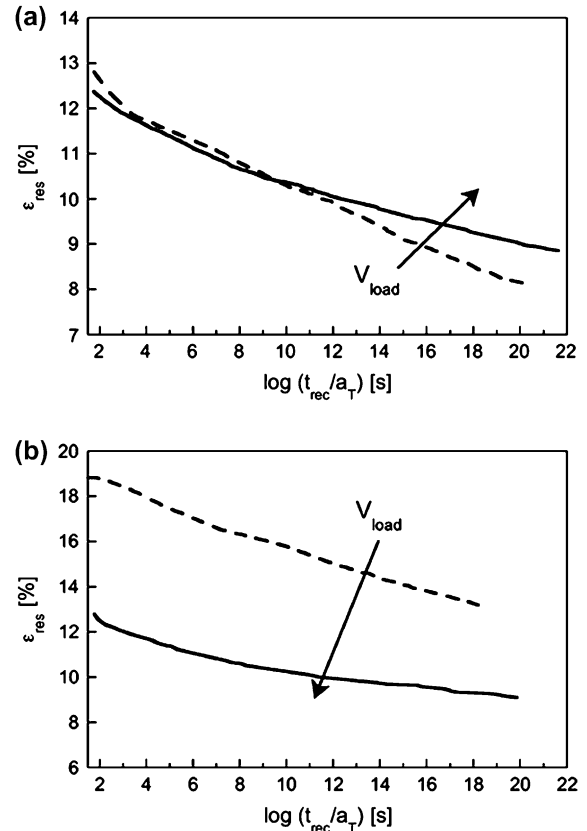


Fig. 4. Strain recovery master curves, for specimens deformed up to $\epsilon_0 = 30\%$, at $V_{load} = 10$ mm/min (solid lines) or $V_{load} = 0.05$ mm/min (dotted lines) obtained at (a) $T_{def} = T_{ref} = 45$ °C, and (b) $T_{def} = T_{ref} = 100$ °C.

deformed at $T_{\text{def}} = 25\text{ }^{\circ}\text{C}$, with a more rapid kinetics for *slowly* deformed specimens in comparison to *quickly* deformed ones.

It is now interesting to directly compare all the master curves obtained at different T_{def} by referring them to the same temperature, for example $T_{\text{ref}} = 25\text{ }^{\circ}\text{C}$, as reported in Fig. 5. The comparison clearly excludes the possibility to consider any recovery time–deformation temperature superposition, thus evidencing different mechanisms underlying recovery of specimens deformed at temperatures below or above their glass transition temperature.

All master curves display a reduction of the strain recovery rate for long times, and the completion of the recovery process has never been reached under the analysed conditions. The impossibility to have a full strain recovery is confirmed by the presence of an irreversible deformation component in the specimens. It is important to underline that this irreversible strain component is not usually observed on amorphous polymers deformed in the glassy state. The presence of an irreversible strain component in semicrystalline PBT, is therefore to be attributed to the crystalline phase, which could be permanently deformed and also decreases the mobility of the chains in the amorphous regions and eventually hinders their complete reversion to the original state.

The values of the irreversible strain component are reported in Fig. 6 as a function of the deformation temperature for specimens *quickly* or *slowly* deformed up to 30% strain. It is worthwhile to note that this strain component increases as the deformation temperature increases. Moreover, also the strain rate has an effect on the irreversible strain. In fact, when deforming specimens at temperatures below the glass transition temperature a slightly lower irreversible strain value can be found for the *slow* deformation (the same strain rate dependence is also observed for specimens deformed at 15% strain). When specimens are deformed at $T_{\text{def}} = T_g$ the irreversible strain component seems to be independent of the deformation rate, whereas when specimens are deformed well above T_g ($T_{\text{def}} = 100\text{ }^{\circ}\text{C}$) such a component is lower for specimens *quickly* deformed. This effect is probably related to the

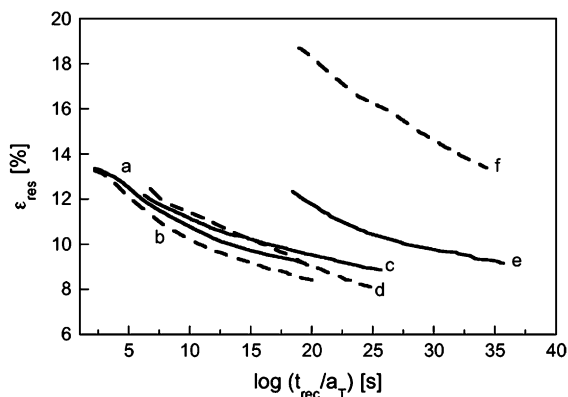


Fig. 5. Strain recovery master curves at $T_{\text{ref}} = 25\text{ }^{\circ}\text{C}$ for samples deformed up to $\varepsilon_0 = 30\%$, and (a) $T_{\text{def}} = 25\text{ }^{\circ}\text{C}$, $V_{\text{load}} = 10\text{ mm/min}$; (b) $T_{\text{def}} = 25\text{ }^{\circ}\text{C}$, $V_{\text{load}} = 0.05\text{ mm/min}$; (c) $T_{\text{def}} = 45\text{ }^{\circ}\text{C}$, $V_{\text{load}} = 10\text{ mm/min}$; (d) $T_{\text{def}} = 45\text{ }^{\circ}\text{C}$, $V_{\text{load}} = 0.05\text{ mm/min}$; (e) $T_{\text{def}} = 100\text{ }^{\circ}\text{C}$, $V_{\text{load}} = 10\text{ mm/min}$; and (f) $T_{\text{def}} = 100\text{ }^{\circ}\text{C}$, $V_{\text{load}} = 0.05\text{ mm/min}$.

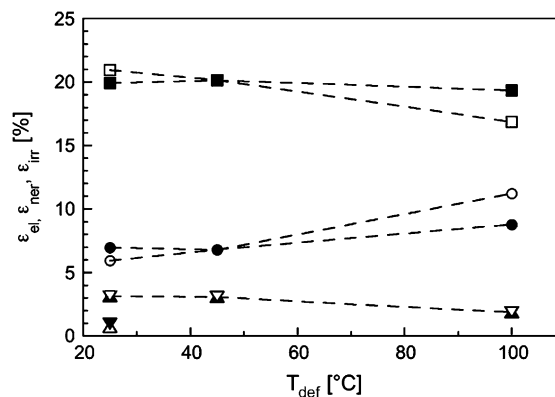


Fig. 6. Effect of the deformation temperature on the strain components of specimens deformed up to 30%: elastic component at (▲) $V_{\text{load}} = 10\text{ mm/min}$ and (▼) $V_{\text{load}} = 0.05\text{ mm/min}$; non-elastic reversible component at (■) $V_{\text{load}} = 10\text{ mm/min}$ and (□) $V_{\text{load}} = 0.05\text{ mm/min}$; irreversible component at (●) $V_{\text{load}} = 10\text{ mm/min}$ and (○) $V_{\text{load}} = 0.05\text{ mm/min}$. Irreversible component for samples deformed at room temperature up to 15% at (▼) $V_{\text{load}} = 10\text{ mm/min}$ and (△) $V_{\text{load}} = 0.05\text{ mm/min}$.

occurrence of a viscous flow, and to the longer times under load in case of a slow deformational process.

The elastic and non-elastic reversible components are also represented in Fig. 6. It shows that the elastic component slightly decreases with deformation temperature, with no apparent dependence on the strain rate. Concurrently, the non-elastic reversible component is found to decrease with the deformation temperature for sample deformed at low strain rate, whereas it is almost constant for high strain rate. However, this component is higher for the lower strain rate when specimens are deformed at room temperature, while at temperatures far above T_g a lower strain rate leads to lower non-elastic reversible component.

For amorphous glassy polymers the features of the recovery behaviour have been explained by Perez et al. in the framework of a so-called crystal-like approach [27,58]. For stresses applied at temperatures below the glass transition, plastic strain is supposed to nucleate as shear micro-domains (SMD) arising in correspondence of points of fluctuation in the local free volume of the amorphous matrix called quasi-point defects (QPD). According to Oleinik [11], generated defects can relax either reverting to their initial state or by recombination between each other at the boundary, releasing the energy stored and transforming into a micro-defect with different nature but almost the same energy level. The presence of two different types of defects leads to two different recovery mechanisms, distinguished on the time scale: QPD feature recovery for shorter times when the driving force is the energy stored at the defects border; recombined QPD may also induce recovery at longer times on the driving force of the configuration entropy. Further, works on deformational behaviour of semicrystalline materials [48–50] showed that, at progressively increasing strain levels, different crystallite texture changes take place simultaneously. These changes are associated with inter- and intralamellar slip processes, fragmentation of the lamellar crystals and chain

disentanglement, depending on the applied deformation and involving different microstructural levels. Therefore, the effects of the various deformation conditions (temperature and rate) on the various strain components, reported in Fig. 6, are rather complex to be analysed and its explanation requires further investigations.

3.2. Recovery kinetics of the non-elastic reversible component

Following an approach proposed by other researchers [11,27,29], the derivative $d\epsilon_{res}/d\log(t_{rec})$ of the recovery master curve has been analysed, in order to obtain information on the times distribution of the recovery process. For amorphous polymers deformed in the glassy state, the recovery rate distributions usually show two distinct peaks, associated to different strain components [11,27,29]. In the present case, as shown in Fig. 7 for the samples deformed at $T_{def}=25\text{ }^\circ\text{C}$ at various strain levels and strain rates, only one recovery peak can be detected. As a consequence, a single reversible strain component can be identified on a time basis. The recovery rate markedly increases as the deformation level increases. Moreover, the recovery rate increases as the deformation rate decreases.

As evidenced in Fig. 8, the derivatives of the master curves markedly depend on the deformation temperature and rate. In fact, quickly deformed samples begin their recovery process with higher rate when deformed at elevated temperature, and the recovery rate progressively diminishes down to converge to the same recovery rate independently of the deformation temperature. On the other hand, the recovery rate of slowly deformed samples does not converge to a same value at elevated recovery time, but they display higher values for samples deformed at higher temperatures.

The shift factors adopted for the construction of master curves of Figs. 3 and 4 are all reported in Fig. 9a as a function of the reciprocal of the absolute temperature. The apparent linearity of the experimental data is suggesting the applicability

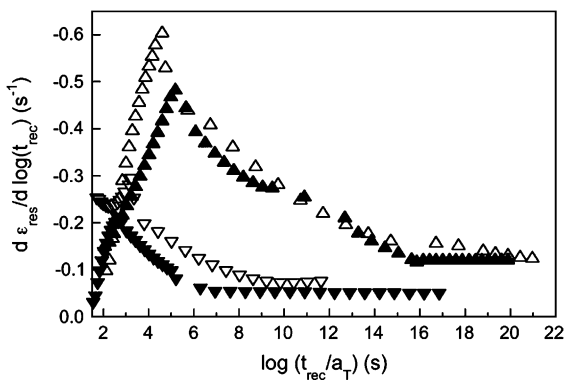


Fig. 7. Derivative of the residual deformation $d\epsilon_{res}/d\log(t_{rec})$ of the recovery master curves of samples deformed at (▼) $T_{def}=25\text{ }^\circ\text{C}$, $V_{load}=10\text{ mm/min}$, $\epsilon_0=15\%$; (▽) $T_{def}=25\text{ }^\circ\text{C}$, $V_{load}=0.05\text{ mm/min}$, $\epsilon_0=15\%$; (▲) $T_{def}=25\text{ }^\circ\text{C}$, $V_{load}=10\text{ mm/min}$, $\epsilon_0=30\%$; and (Δ) $T_{def}=25\text{ }^\circ\text{C}$, $V_{load}=0.05\text{ mm/min}$, $\epsilon_0=30\%$.

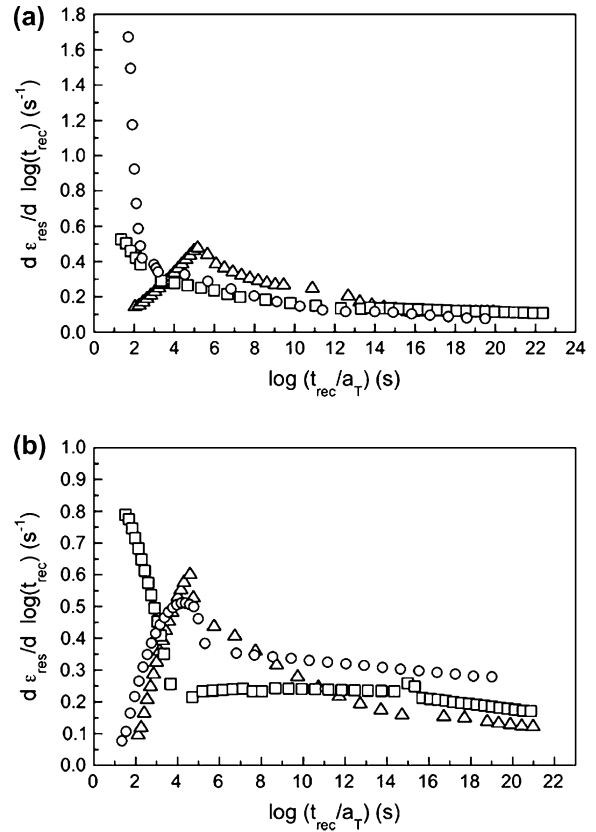


Fig. 8. Derivative of the residual deformation $d\epsilon_{res}/d\log(t_{rec})$ of the recovery master curves of samples deformed at $\epsilon_0=30\%$, at (Δ) $T_{def}=25\text{ }^\circ\text{C}$; (□) $T_{def}=45\text{ }^\circ\text{C}$; and (○) $T_{def}=100\text{ }^\circ\text{C}$. (a) $V_{load}=10\text{ mm/min}$, and (b) $V_{load}=0.05\text{ mm/min}$.

of an Arrhenius equation for the temperature dependence of the shift factors, which can be written in the following form:

$$a_T = A \exp\left(-\frac{E_a}{RT}\right) \quad (2)$$

where A is a constant, E_a is an activation energy, R is the universal gas constant, and T is the absolute temperature. The activation energy values of the strain recovery process, evaluated on the basis of the linear regression of the shift factors, are reported in Fig. 9b, as a function of the deformation temperature. The results indicate that the specimens deformed at the same temperature ($25\text{ }^\circ\text{C}$) display more or less the same activation energy independently from the deformation level ϵ_0 and that the activation energy has a tendency to increase with the deformation temperature. It is worthwhile to note that this increase with temperature is associated with a decrease of the deformation energy stored in the material, as obtained by calorimetric measurements [21].

3.3. Analysis of fractional recovery

To deepen the understanding of the recovery process and its dependence on the deformation conditions, the recovery master curves can be represented as the strain recovery level evaluated at different times after unloading as a function of

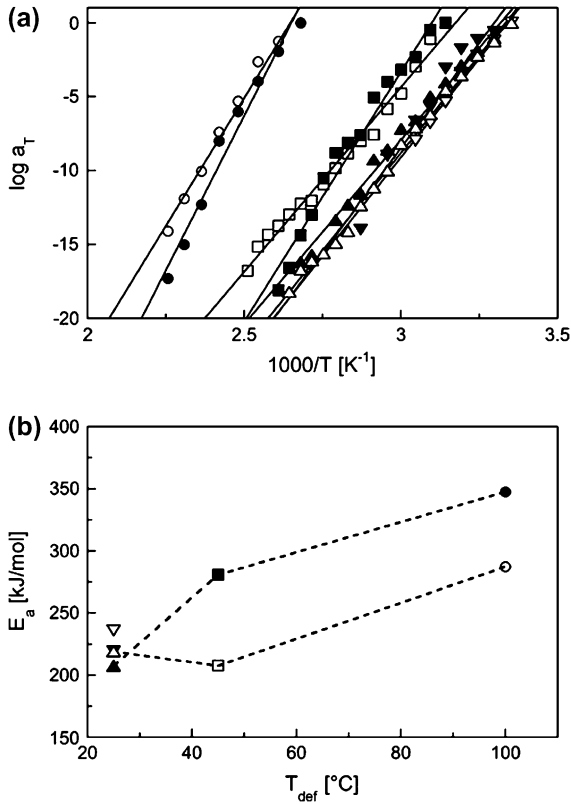


Fig. 9. Shift factors (a) and activation energy values (b) for the strain recovery master curves obtained at: (\blacktriangledown) $T_{def} = 25$ °C, $V_{load} = 10$ mm/min, $\epsilon_0 = 15\%$; (∇) $T_{def} = 25$ °C, $V_{load} = 0.05$ mm/min, $\epsilon_0 = 15\%$; (\blacktriangle) $T_{def} = 25$ °C, $V_{load} = 10$ mm/min, $\epsilon_0 = 30\%$; (\triangle) $T_{def} = 25$ °C, $V_{load} = 0.05$ mm/min, $\epsilon_0 = 30\%$; (\blacksquare) $T_{def} = 45$ °C, $V_{load} = 10$ mm/min, $\epsilon_0 = 30\%$; (\square) $T_{def} = 45$ °C, $V_{load} = 0.05$ mm/min, $\epsilon_0 = 30\%$; (\bullet) $T_{def} = 100$ °C, $V_{load} = 10$ mm/min, $\epsilon_0 = 30\%$; (\circ) $T_{def} = 100$ °C, $V_{load} = 0.05$ mm/min, $\epsilon_0 = 30\%$.

the deformation temperature. In fact, this approach permits to better analyse how each step of the recovery process takes place along time, and to compare the recovery of specimens deformed at different temperatures at the same strain rate. The recovery level at a certain instant can be conveniently expressed as a fractional recovery, defined as [51]:

$$\text{fractional recovery} = \frac{\epsilon_0 - \epsilon_{res}(t)}{\epsilon_0} \quad (3)$$

For both the investigated deformation rates, fractional recovery data are represented in Fig. 10, for recovery times ranging from 10 min to 10¹⁸ min, which represent a significant portion of the experimental window. These plots are displayed with three additional curves: (i) the elastic fractional recovery curve, which represents the percentage of the deformation recovered instantaneously as obtained by Eq. (3) evaluated for $\epsilon_{res}(t) = \epsilon_0 - \epsilon_{el}$; (ii) the residual fractional recovery curve at unloading, which represents the fractional recovery at the end of the unloading step (Eq. (3) evaluated for $\epsilon_{res}(t) = \epsilon_{res0}$); and (iii) the irreversible fractional recovery curve, representing the maximum fractional recovery (from Eq. (3) for $\epsilon_{res}(t) = \epsilon_{irr}$). These curves (i, ii, iii) have been added in order to complete the data taken from the recovery master curves with data lying outside the experimental window of the recovery tests,

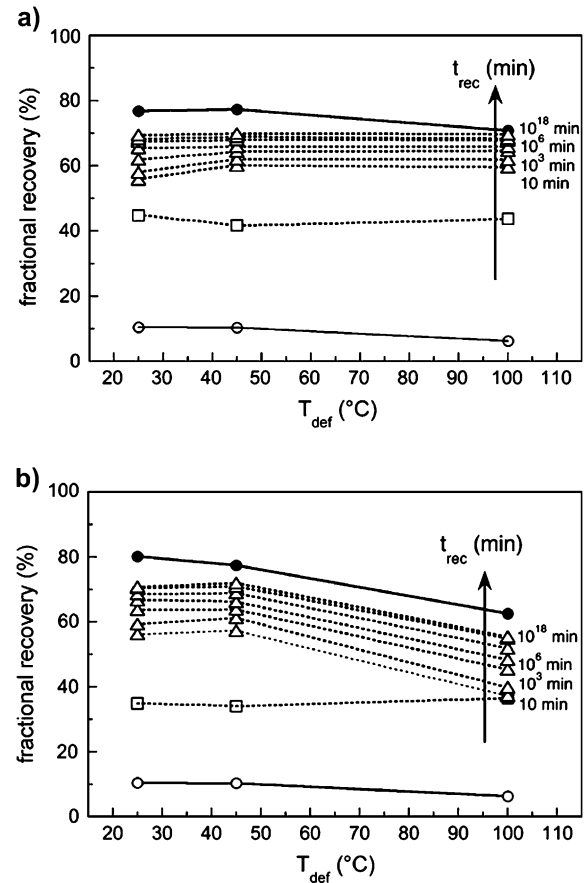


Fig. 10. Fractional recovery versus deformation temperature for specimens deformed at a deformation level $\epsilon_0 = 30\%$. (a) $V_{load} = 10$ mm/min, and (b) $V_{load} = 0.05$ mm/min; (\triangle) data from recovery master curve for $T_{rec} = 10$, 10³, 10⁶, 10⁹, 10¹², 10¹⁵, 10¹⁸ s; (\circ) elastic fractional recovery (referred to $\epsilon_{res}(t) = \epsilon_0 - \epsilon_{el}$); (\square) residual fractional recovery at unloading (referred to $\epsilon_{res}(t) = \epsilon_{res0}$); (\bullet) irreversible fractional recovery ($\epsilon_{res}(t) = \epsilon_{irr}$).

corresponding to the elastic recovery, and to the beginning and the end of the whole non-elastic recovery process, respectively. From these curves, we can see that for both strain rates the elastically recovered deformation is approximately only a tenth of the total applied deformation, whereas a large part of the non-elastic recovery actually takes place during the unloading stage, with a larger recovery percentage for samples deformed at a fast rate (Fig. 10a) than those deformed at a slow rate (Fig. 10b), and with no significant dependence on the deformation temperature. Further, for all the specimens deformed at the fast deformation rate another relevant part of the recovery process takes place in the first 10 min after unloading, and this part is larger for samples deformed at higher temperatures. Specimens deformed at a slow strain rate show a similar behaviour only for the deformation temperatures below or close to T_g , with a slight increase of this recovery fraction with the deformation temperature, but for deformation temperatures above T_g , no significant recovery is exhibited in the first 10 min after unloading.

Moreover, it is noteworthy to observe that at each deformation temperature specimens *quickly* deformed exhibit in the first 10 min a larger recovery than *slowly* deformed specimens.

This result seems to indicate that a higher strain rate provides generally a less stable deformed state.

The comparison between the results reported in Fig. 10a and b permits therefore a better understanding of the anomalous behaviour displayed by the recovery master curves for samples slowly deformed above T_g (see Fig. 4b). In fact, these results highlight that in the case of specimens slowly deformed above T_g the recovery master curve starts from a higher residual deformation value since the time interval associated to the master curve (10 min – 10^{18} min) permits to investigate only residual deformation values closer to the “initial” part of the recovery process, whereas for samples *quickly* deformed above T_g the same time window allows one to have information only on the residual deformations closer to the “final” part of the recovery process. These considerations also justify the presence of a peak in the strain recovery derivative curve for the specimens slowly deformed above T_g , which is not displayed by the curves of quickly deformed specimens. This peak is related to the characteristic time at which the recovery process becomes significantly fast. Thus, its absence in quickly deformed specimen indicates that a faster recovery takes place actually in the first 10 min. The more stable structure of slowly deformed specimens requires longer times for the process to become relevant, and permits to detect this peak in our recovery tests.

4. Conclusions

The isothermal strain recovery behaviour of semicrystalline PBT has been studied for various recovery temperatures on specimens compressed up to post-yield deformation levels under various deformation conditions. By contrast with what is commonly found in amorphous polymers deformed in the glassy state, the recovery process extends up to temperatures far above the material glass transition and an irreversible deformation component is found. The amount of unrecoverable deformation, ε_{irr} , depends on deformation temperature and strain rate. In particular, it increases with deformation temperature both at slow and high rates. Further, at deformation temperature below T_g , ε_{irr} is lower for slowly deformed specimen than for those deformed at the higher strain rate, whereas above T_g a higher unrecoverable strain is found for slowly deformed specimen.

The strain recovery master curves show that when deformation takes place at room temperature the residual deformation values are lower for *slowly* deformed specimen. When deformation temperature approaches T_g , the master curves for slow and fast deformation rates are quite similar. When deformation temperature is well above T_g the residual deformation level at each recovery time is lower for *quickly* deformed specimen.

It is worthwhile to note that an amount of deformation ranging between 35% and 45% is recovered already in the unloading stage for each deformation temperature, and this amount seems to be slightly higher when the deformation rate is fast. After the first 10 min after unloading, sample deformed below and close to T_g presents a further recovery of approximately 10–20% of the total deformation, with small

differences between the two strain rates. By contrast, for deformation temperature above T_g specimens deformed at slow and fast strain rates show quite different behaviour in the first part of the recovery process. In particular, specimen deformed with a fast rate recovers a large part of the residual deformation in the first 10 min after unloading, whereas, in the same time interval, the recovery process of specimen *slowly* deformed takes place in a slower manner and the total recovery time related to the non-elastic component appears longer.

References

- [1] Entgelter Ad, Müller FH. Kolloid Zeitschrift 1958;157(2):89–111.
- [2] Park JB, Uhlmann DR. Journal of Applied Physics 1973;44(1):201–6.
- [3] Kung T-M, Li JCM. Journal of Polymer Science, Part B: Polymer Physics 1986;24:2433–45.
- [4] Kung T-M, Li JCM. Journal of Materials Science 1987;22:3620–30.
- [5] Chang BT, Li JCM. Polymer Engineering and Science 1988;28(18):1198–202.
- [6] Salamatina OB, Nazarenko SI, Rudnev SN, Oleinik EF. Mekhanika Kompozitnykh Materialov 1988;6:979–84.
- [7] Oleinik EF. Progress in Colloid and Polymer Science 1989;80:140–50.
- [8] G'Sell C, El Bari H, Perez J, Cavaille JY, Johari GP. Materials Science and Engineering, A: Structural Materials: Properties, Microstructure and Processing 1989;A110:223–9.
- [9] Adams GW, Farris RJ. Polymer 1989;30:1824–8.
- [10] Rudnev SN, Salamatina OB, Voenniy VV, Oleinik EF. Colloid and Polymer Science 1991;269:460–8.
- [11] Oleinik EF. Distortional plasticity of organic glassy polymers. In: Baer E, Moet A, editors. High performance polymers: structure, properties, composites, fibers. Munich: Hanser Publishers; 1991. p. 79–102.
- [12] Godovsky YK. Thermodynamic behavior of solid polymers in plastic deformation and cold drawing. Thermophysical properties of polymers. Berlin: Springer-Verlag; 1992. p. 211–48.
- [13] Salamatina OB, Rudnev SN, Voenniy VV, Oleinik EF. Journal of Thermal Analysis 1992;38:1271–81.
- [14] Hasan OA, Boyce MC. Polymer 1993;34:5085–92.
- [15] Oleinik EF, Salamatina OB, Rudnev SN, Shenogin SV. Vysokomolekulyarnye Soedineniya, Seriya A 1993;35(11):1532–58.
- [16] Salamatina OB, Höhne GWH, Rudnev SN, Oleinik EF. Thermochimica Acta 1994;247:1–18.
- [17] Oleinik EF, Salamatina OB, Rudnev SN, Shenogin SV. Polymers for Advanced Technologies 1995;6:1–9.
- [18] Boyce MC, Haward RN. The post-yield deformation of glassy polymers. In: Haward RN, Young RJ, editors. The physics of glassy polymers - 2nd ed. London: Chapman & Hall; 1997. p. 213–93.
- [19] Pegoretti A, Guardini A, Migliaresi C, Ricco T. Polymer 2000;41(5):1857–64.
- [20] Ricco T, Pegoretti A. Journal of Polymer Science, Part B: Polymer Physics 2002;40(2):236–43.
- [21] Pegoretti A, Pandini S, Ricco T. Polymer 2004;45(8):2759–67.
- [22] Park JB, Uhlmann DR. Journal of Applied Physics 1970;41(7):2928–35.
- [23] Park JB, Uhlmann DR. Journal of Applied Physics 1971;42(10):3800–5.
- [24] Li JC-M. Metallurgical Transactions A: Physical Metallurgy and Materials Science 1978;9A:1353–80.
- [25] Adams GW, Farris RJ. Polymer 1989;30:1829–35.
- [26] Bordonaro CM, Krempel E. Polymer Engineering and Science 1992;32(16):1066–72.
- [27] Quinson R, Perez J, Rink M, Pavan A. Journal of Materials Science 1996;31:4387–94.
- [28] Tanaka N. Journal of Thermal Analysis 1996;46:1021–31.
- [29] David L, Quinson R, Gauthier C, Perez J. Polymer Engineering and Science 1997;37:1633–40.

- [30] Quinson R, Perez J, Rink M, Pavan A. *Journal of Materials Science* 1997; 32:1371–9.
- [31] Charoensirisomboon P, Saito H, Inoue T, Oishi Y, Mori K. *Polymer* 1998; 39(11):2089–93.
- [32] Iwasa N, Yoshioka S, Nanzai Y. *Materials Science Research International* 1998;4(2):103–7.
- [33] Aoyama T, Carlos AJ, Saito H, Inoue T, Niitsu Y. *Polymer* 1999;40(13): 3657–63.
- [34] Pegoretti A, Guardini A, Migliaresi C, Ricco T. *Journal of Applied Polymer Science* 2000;78(9):1664–70.
- [35] D’Aniello C, Romano G, Russo R, Vittoria V. *European Polymer Journal* 2000;36:1571–7.
- [36] Sun N, Yuan Z, Yang J, Shen D. *Journal of Macromolecular Science, Physics* 2000;B39(3):397–405.
- [37] Meyer RW, Pruitt LA. *Polymer* 2001;42(12):5293–306.
- [38] Volynskii AL, Keчек’yan AS, Grokhovskaya TE, Lyulevich VV, Bazhenov SL, Ozerin AN, et al. *Polymer Science Series A* 2002;44(4): 374–85.
- [39] Bendler JT, LeGrand DG, Olszewski WV. *Polymer* 2002;43(2):389–94.
- [40] Chau CC, Li JCM. *Polymer* 2003;44(12):3545–51.
- [41] Gauthier C. Recovery of glassy polymers. In: Swallowe GM, editor. *Mechanical properties and testing of polymers – an A–Z reference*. Dordrecht (The Netherlands): Kluwer Academic Publishers; 1999. p. 191–4.
- [42] Russell TP, Brown HR. *Journal of Polymer Science, Part B: Polymer Physics* 1987;25:1129–48.
- [43] Bartczak Z, Cohen RE, Argon AS. *Macromolecules* 1992;25(18): 4692–704.
- [44] Bartczak Z, Argon AS, Cohen RE. *Macromolecules* 1992;25(19): 5036–53.
- [45] Galeski A, Bartczak Z, Argon AS, Cohen RE. *Macromolecules* 1992; 25(21):5705–18.
- [46] Lin A, Argon AS. *Journal of Materials Science* 1994;29(2):294–323.
- [47] Boontongkong Y, Cohen RE, Spector M, Bellare A. *Polymer* 1998; 39(25):6391–400.
- [48] Hiss R, Hobeika S, Lynn C, Strobl G. *Macromolecules* 1999;32(13): 4390–403.
- [49] Hobeika S, Men Y, Strobl G. *Macromolecules* 2000;33(5):1827–33.
- [50] Fu Q, Men Y, Strobl G. *Polymer* 2003;44(6):1927–33.
- [51] Moore DR, Turner S. *Mechanical evaluation strategies for plastics*. Cambridge (UK): Woodhead Publishing Limited; 2001. p. 113.
- [52] Nanzai Y. *Progress in Polymer Science*; 1993.
- [53] Stachurski ZH. *Progress in Polymer Science* 1997;22(3):407–74.
- [54] Arruda EM, Boyce MC, Jayachandran R. *Mechanics of Materials* 1995; 19(2–3):193–212.
- [55] <http://www.dow.com/sal/design/guide/thermal.htm>; [last accessed November 2005].
- [56] Struik LCE. *Physical ageing in amorphous polymers and others material*. Amsterdam: Elsevier; 1978.
- [57] Zhao J, Wang JJ, Li CX, Fan QR. *Macromolecules* 2002;35(8):3097–103.
- [58] Perez J. *Physique et mecanique des polymers amorphes*. Paris: Lavoisier; 1992.